

AD-A073 373

DAYTON UNIV OHIO
COMPRESSIVE STRENGTH CHARACTERISTICS OF THE PRIMATE 'MACACA MUL--ETC(U)
MAY 79 L F KAZARIAN, & GRAVES

F/G 6/19
F33615-76-C-5008
NL

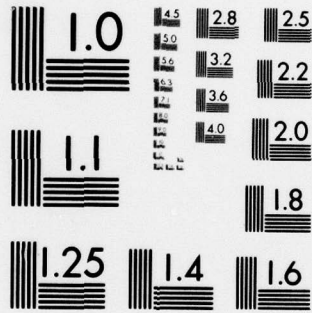
UNCLASSIFIED

AMRL-TR-79-8

| OF |
AD
A073373



END
DATE
FILMED
9-79
DDC



MICROCOPY RESOLUTION TEST CHART
NATIONAL BUREAU OF STANDARDS-1963-A

① 12 LEVEL II 86

AMRL-TR-79-8



**COMPRESSIVE STRENGTH CHARACTERISTICS
OF THE PRIMATE (MACACA MULATTA)
VETEBRAL CENTRUM**

LEON E. KAZARIAN
AEROSPACE MEDICAL RESEARCH LABORATORY

GEORGE GRAVES
UNIVERSITY OF DAYTON
DAYTON, OHIO 45409

May 1979

DDC
RECEIVED
SEP 11 1979
B

Approved for public release; distribution unlimited.

AEROSPACE MEDICAL RESEARCH LABORATORY
AEROSPACE MEDICAL DIVISION
AIR FORCE SYSTEMS COMMAND
WRIGHT-PATTERSON AIR FORCE BASE, OHIO 45433

79 09 10 023

AD A 073373

DDC FILE COPY

NOTICES

When US Government drawings, specifications, or other data are used for any purpose other than a definitely related Government procurement operation, the Government thereby incurs no responsibility nor any obligation whatsoever, and the fact that the Government may have formulated, furnished, or in any way supplied the said drawings, specifications, or other data, is not to be regarded by implication or otherwise, as in any manner licensing the holder or any other person or corporation, or conveying any rights or permission to manufacture, use, or sell any patented invention that may in any way be related thereto.

Please do not request copies of this report from Aerospace Medical Research Laboratory. Additional copies may be purchased from:

National Technical Information Service
5285 Port Royal Road
Springfield, Virginia 22161

Federal Government agencies and their contractors registered with Defense Documentation Center should direct requests for copies of this report to:

Defense Documentation Center
Cameron Station
Alexandria, Virginia 22314

TECHNICAL REVIEW AND APPROVAL

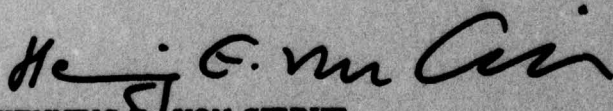
AMRL-TR-79-8

The experiments reported herein were conducted according to the "Guide for the Care and Use of Laboratory Animals," Institute of Laboratory Animal Resources, National Research Council.

This report has been reviewed by the Information Office (OI) and is releasable to the National Technical Information Service (NTIS). At NTIS, it will be available to the general public, including foreign nations.

This technical report has been reviewed and is approved for publication.

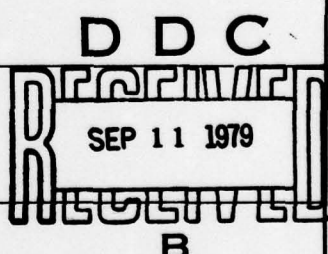
FOR THE COMMANDER



HENNING E. VON GIERKE

Director

Biodynamics and Bioengineering Division
Aerospace Medical Research Laboratory

19 REPORT DOCUMENTATION PAGE		READ INSTRUCTIONS BEFORE COMPLETING FORM
1. REPORT NUMBER 18 AMRL TR-79-8	2. GOVT ACCESSION NO.	3. RECIPIENT'S CATALOG NUMBER
6 TITLE (and Subtitle) COMPRESSIVE STRENGTH CHARACTERISTICS OF THE PRIMATE (MACACA MULATTA) VERTEBRAL CENTRUM		5 TYPE OF REPORT & PERIOD COVERED Technical Report
10 AUTHOR(s) Leon E. Kazarian George Graves		6 PERFORMING ORG. REPORT NUMBER
9. PERFORMING ORGANIZATION NAME AND ADDRESS Aerospace Medical Research Laboratory, Aerospace Medical Division, Air Force Systems Command, Wright-Patterson Air Force Base, Ohio 45433		8. CONTRACT OR GRANT NUMBER(s) F33615-76-C-5008 new
11. CONTROLLING OFFICE NAME AND ADDRESS		10. PROGRAM ELEMENT, PROJECT, TASK AREA & WORK UNIT NUMBERS 62202F, 2312-V3-12
14. MONITORING AGENCY NAME & ADDRESS (if different from Controlling Office)		12. REPORT DATE 11 May 1979
		13. NUMBER OF PAGES 53
		15. SECURITY CLASS. (of this report) Unclassified (12) 53 P.
16. DISTRIBUTION STATEMENT (of this Report) Approved for Public Release; distribution unlimited		15a. DECLASSIFICATION/DOWNGRADING SCHEDULE
17. DISTRIBUTION STATEMENT (of the abstract entered in Block 20, if different from Report)		
18. SUPPLEMENTARY NOTES *University of Dayton Dayton, Ohio 45409		
19. KEY WORDS (Continue on reverse side if necessary and identify by block number) Spinal Biomechanics Tissue Strength Macaca Mulatta Orthopaedics		
20 ABSTRACT (Continue on reverse side if necessary and identify by block number) A two-phase experiment was conducted on isolated normal vertebral bodies excised from the Rhesus Macaque at necropsy. The purpose of this experiment was to evaluate the effects of displacement rate and vertebral body position on mechanical properties. The first phase of the experimental tests was performed as a factorial experiment in which 12 vertebrae from each of four monkeys were loaded and mechanically strained at each of three displacement rates. The objective of this phase was to determine the effect of these factors on seven mechanical properties and to determine the appropriate		

DD FORM 1 JAN 73 1473 EDITION OF 1 NOV 65 IS OBSOLETE

105 350

JOB

regression model for describing vertebral body response. In the second phase an additional 48 vertebrae were tested at three different intermediate displacement rates other than those of Phase I, again for the various vertebral body positions and according to a factorial arrangement of treatment combination. The results from Phase II were compared to Phase I. The data from the two phases were combined and the parameters of the regression model were estimated for each of the mechanical properties.



SUMMARY

A two-phase compression experiment was conducted on 96 freshly excised Rhesus monkey vertebral bodies. The purpose of the tests was to evaluate the effects of displacement rate and vertebral body position on mechanical properties. The objective of the first phase was to determine the effect of displacement rate and vertebral body position on seven measured mechanical properties. The appropriate regression model for describing the responses on 48 vertebrae was derived. In the second phase an additional 48 vertebrae were tested at three different displacement rates for vertebral body position according to a factorial arrangement of treatment combination. The results from Phase II were compared to those of Phase I. The data from the two phases were combined and the parameters of the regression model were estimated for each of the mechanical properties.

ACCESSION for	
NTIS	White Section <input checked="" type="checkbox"/>
DDC	Buff Section <input type="checkbox"/>
UNANNOUNCED	<input type="checkbox"/>
JUSTIFICATION _____	
BY _____	
DISTRIBUTION/AVAILABILITY CODES	
Dist. AVAIL. and/or SPECIAL	
A	

CONTENTS

	<i>Page</i>
INTRODUCTION	5
METHODS	5
Test Specimen Preparation and Procedures	6
The Test System	7
Data Reduction Methodology	7
Statistical Analysis	8
RESULTS AND DISCUSSIONS	14
Ultimate Load	14
Deformation to Ultimate Load	15
Stiffness	17
Energy to Ultimate Load	22
Ultimate Engineering Stress	24
Engineering Strain to Ultimate Stress	26
Elastic Modulus	29
The Regression Model	33
APPENDIX I	42
APPENDIX II	45
REFERENCES	49

LIST OF ILLUSTRATIONS

<i>Figure</i>		<i>Page</i>
1	Superior View of a Vertebral Body From the Rhesus Monkey on the Left, Human on the Right (Note position of the transverse process.)	6
2	Vertebral Body with its Acrylic Bearing Surfaces Just Prior to Test	7
3	A Typical Load versus Displacement Test Curve	8
4	Average Ultimate Load for Position by Displacement Rate Combinations	14
5	Average Deformation to Ultimate Load for Position by Displacement Rate Combinations	15
6	Stiffness for Position by Displacement Rate Combinations	19
7	Average Energy to Ultimate Load for Position by Displacement Rate Combinations	22
8	Average Ultimate Engineering Stress for Position by Displacement Rate Combinations	25
9	Average Engineering Strain to Ultimate for Position by Displacement Rate Combinations	28
10	Average Elastic Modulus for Position by Displacement Rate Combinations	29
11	Regression Results for Stress vs. Displacement Rate — P ₁	35
12	Regression Results for Deformation vs. Displacement Rate — P ₁	36
13	Regression Results for Stiffness vs. Displacement Rate — (P ₁ and P ₂)	37
14	Regression Results for Energy vs. Displacement Rate — P ₁	38
15	Regression Results for Stress vs. Displacement Rate — All Positions	39
16	Regression Results for Strain vs. Displacement Rate — P ₁ and P ₂	40
17	Regression Results for Elastic Modulus vs. Displacement Rate — P ₁	41

PREFACE

The research reported in this paper was sponsored and performed by the Aerospace Medical Research Laboratory, Aerospace Medical Division, Air Force Systems Command, Wright-Patterson Air Force Base, Ohio, in part under Contract No. F3361576-C-5008. The experiments were conducted in support of Project 2312V312, "Comparative Response of Man and Animals to Mechanical Stress."

✓	SEARCHED	INDEXED
	SERIALIZED	FILED
OCT 1968		
AFMRL		
WRIGHT-PATTERSON AIR FORCE BASE, OHIO		
RESEARCH REPORT		
NO. 2312V312		
TITLE		
AUTHOR		
SUBJECT		
DISTRIBUTION STATEMENT		
AVAILABILITY STATEMENT		
SECURITY CLASSIFICATION		
UNCLASSIFIED		
DATE		
BY		
REMARKS		
A		

LIST OF TABLES

<i>Table</i>		<i>Page</i>
1	Test Matrix for Vertebral Body Compression Tests (R = Strain Rate, S = Subject, P = Spinal Position)	10
2	General Analysis of Variance Table for Vertebral Body Testing Data	11
3	Phase I — Ultimate Load (N) And Analysis of Variance Table	12
4	Phase II Results — Ultimate Loads (N)	13
5	Phase I Results — Deformation to Ultimate Load ($m \times 10^{-3}$) — Analysis of Variance Table	16
6	Phase II Results — Deformation to Ultimate Load ($m \times 10^{-3}$)	17
7	Phase I Results — Stiffness ($N/m \times 10^6$) Analysis of Variance Table	18
8	Phase II Results — Stiffness ($N/m \times 10^6$)	20
9	Phase I Results — Energy to Ultimate Load (J) Analysis of Variance Table	21
10	Phase II Results — Energy to Ultimate Load (J)	23
11	Phase I Results — Ultimate Engineering Stress ($P_a \times 10^6$) — Analysis of Variance Table	24
12	Phase II Results — Ultimate Engineering Stress ($P_a \times 10^6$)	26
13	Phase I Results — Engineering Strain to Ultimate Stress (m/m)	27
14	Phase II Results — Engineering Strain to Ultimate Stress (m/m)	30
15	Phase I Results — Elastic Modulus ($P_a \times 10^6$)	31
16	Phase II Results — Elastic Modulus ($P_a \times 10^6$)	32
17	Summary of Regression Results for Rhesus Monkeys	33

INTRODUCTION

The concept of a dynamic model representing the axial skeletal system under the influence of a short duration, buttock-to-head acceleration is particularly important when assessing whether or not an arbitrary acceleration time history is tolerable to man. In the study of abrupt accelerative forces and aircrew ejection, attention has focused on the head, spinal column and pelvis. Of these anatomical components, the spinal column has repeatedly been shown to be the most critical to ejection seat forces. Numerous analytical methods for describing and predicting spinal column response have evolved ranging from simple lumped parameter single degree of freedom to multidegree of freedom, to continuum models. The purpose of the models is to ascertain the variation of risk as well as the likelihood of spinal trauma due to various acceleration time histories.

Recent advances in the aerospace sciences have underlined the fact that adequate scientific knowledge dealing with accelerative forces, human spinal response, and injury potential is lacking. The shortcomings of current modeling simulations are obvious. There exists a need for more systematic experimental data collection as a basis for more refined models. Present day modeling efforts are far ahead of the detailed quantitative static and dynamic strength measurements necessary to render analytical modeling efforts useful.

Since the spinal column is composed of discrete components, knowledge of the biomechanical properties of individual tissues is required before a model can be represented as an advanced, discrete, multi-parameter model that simulates and predicts the action of the spine. Data are required in the intervertebral disks, vertebral bodies, ligamentous structures, vertebral units, etc. Because of the relative inaccessibility of human cadaver material for testing and the lack of sufficient quantitative information to adequately describe the operational environments, very limited validation of human response and injury prediction is available using current analytical techniques.

Based upon this information, an investigation was initiated to collect static and dynamic biomechanical strength along with injury mode data to allow the formulation and experimental corroboration of a subhuman primate model. Such an approach would also authenticate the validation of current modeling concepts and practices and may identify the necessary procedures for establishing interspecies scaling relationships that would allow extrapolation of kinesiological, kinetic, and injury potential data between nonhuman primates and man.

This investigation deals with evaluating the effects of displacement rate and vertebral body level on the mechanical properties of isolated vertebral centra excised from the Rhesus monkey [*Macaca mulatta*]. The data presented herein include ultimate load, stiffness of deformation to ultimate load and energy to ultimate load. In this paper, a regression model is estimated for each of the mechanical properties.

METHODS

A two-phase experiment was conducted to evaluate the effects of displacement rate and position on the mechanical properties of isolated Rhesus monkey vertebral bodies. The initial phase was performed as a factorial experiment in which twelve vertebrae from each of four adult Rhesus monkeys were loaded at each of three displacement rates. The objective of this phase was to determine the effect (if any) of these factors on seven measured mechanical properties and to determine the appropriate regression model for describing and predicting the measured responses. In the second phase, an additional 48 vertebrae were tested at three different intermediate displacements other than those in Phase I, again for various vertebral positions according to a factorial arrangement of treatment combinations. The results from Phase II were compared with those of Phase I. The data from the two phases were combined and the parameters of the regression model were estimated for each of the mechanical properties.

The factorial experiment of Phase I consisted of compressive tests on 48 vertebrae from four Rhesus monkeys. The twelve vertebral bodies available from each primate were grouped into four sets of vertebral positions with three vertebrae in each set. Position 1 (P₁) represents vertebra T₈, T₉, and T₁₀; P₂ represents T₁₁, T₁₂ and

L₁; P₃ represents L₂, L₃ and L₄; and P₄ represents L₅, L₆ and L₇. This methodology of grouping assumes that any differences in the mechanical properties of the adjacent vertebrae are negligible in comparison with differences between more distant vertebrae. Each vertebral centrum was subjected to a uniform uniaxial compressive load to failure under a constant displacement rate. Within the respective position groupings, the three assigned vertebrae were tested at one of three displacement rates: R₂ = 8.89 x 10⁻⁵ meters per second, R₄ = 8.89 x 10⁻³ meters pr second, and R₆ = 8.89 x 10⁻¹ meters per second. (R₁ and R₃ and R₅ are intermediate displacement rates and were used for the second phase of this experiment.)

The experiment of Phase II was conducted similarly to that of Phase I. Vertebrae from four different monkeys were subjected to compressive loading under three different displacement rates. The displacement rates were assigned to vertebral position as in Phase I. However, the loading rates in Phase II were set at R₁ = 8.89 x 10⁻⁶ meters/second, R₃ = 8.89 x 10⁻⁴ meters/second and R₅ = 8.89 x 10⁻² meters/second. The objective of this part of the experiment was to demonstrate rates and to provide a larger sample size for estimating the parameters of the model.

TEST SPECIMEN PREPARATION AND PROCEDURES

Eight healthy male Rhesus monkeys [*Macaca mulatta*] were euthanized with an overdose of pentobarbital. The subject identification numbers and body weights are as follows:

X-96	8.1 Kilograms	W92	11.4 Kilograms
884A	10.0 Kilograms	34A	8.8 Kilograms
X90	9.1 Kilograms	584A	8.2 Kilograms
A104	9.3 Kilograms	882A	9.3 Kilograms

Shortly following death, the vertebral columns were excised en masse, identified, and stored in a freezer at -30°C. Thirty-six hours prior to testing, the spinal columns were removed from the deep freeze and allowed to partially thaw. Simultaneously, the individual vertebrae were disarticulated from one another by slicing through the midsection of the intervertebral disks, the articular capsules were sectioned, and the vertebral bodies were separated. The posterior aspects of the vertebral bodies were cut away at the base of the pedicles using a band saw. (In the macaque, the transverse processes of the lumbar and thoracic vertebrae are located on the lateral surface of the vertebral centrum, as shown in Figure 1.) Each vertebral centrum was cleaned of all soft tissue clinging to its surfaces.

All soft tissue was removed from the superior and inferior vertebral body surfaces. The cartilaginous end plate was removed, exposing the bony vertebral surface. Both the superior and inferior vertebral bearing surfaces were pressed into an ink pad and then onto millimeter paper. Vertebral body bearing area was determined for both inferior and superior surfaces, and the results averaged. The length of the vertebral body was measured using vernier calipers.

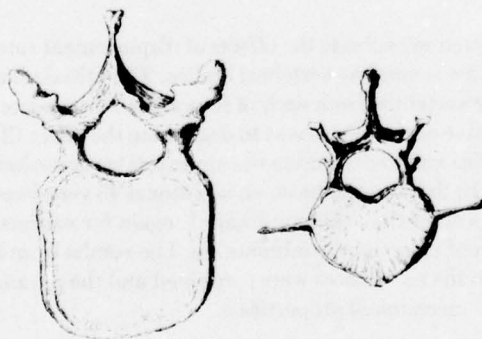


Figure 1. Superior View of a Vertebral Body from the Rhesus Monkey on the Left, Human on the Right (Note position of the transverse process.)

To promote a uniform load distribution, the bearing surfaces of each vertebral centrum were potted in an acrylic compound. Using dental acrylic resin (Acralite 88, Keer Manufacturing Company, Romulus, Michigan), the potting produced circular-shaped pots with the specimen located centrally. The diameter of the pot was subsequently used to locate the center of the specimen coincident with the loading axis of the test machine.

The vertebral centra were pressed into the acrylic at both ends, and the entire assembly was placed in a V-shaped trough to assure that both surfaces were kept parallel and axially aligned as previously described.⁽¹⁾ The vertebral centra was wrapped in a towel soaked in Ringer's solution to prevent drying while the acrylic cured. Figure 2 shows a vertebral body with its acrylic bearing surfaces prepared for test.



Figure 2. Vertebral Body with its Acrylic Bearing Surfaces Just Prior to Test.

THE TEST SYSTEM

An electrohydraulic closed loop test system (Model 810 Material Test System, MTS Systems Corporation, Minneapolis, Minnesota) was used to strain each test specimen. The system is centered around an electrohydraulic closed loop test machine capable of being programmed and controlled in load, strain, and displacement. With the machine in the displacement control mode, a linear ramp function was used to strain each test specimen. Testing was accomplished over five orders of magnitude of linear displacement rates (8.89×10^{-6} m/s to 8.89×10^{-1} m/s). The ultimate ram displacement (specimen deformation) was set at 50% of the original specimen height, up to a maximum of 0.0127 meter. The imposed time dependent displacement and the resultant compression loads were recorded. Ram displacements were measured using a linear variable differential transformer (LVDT), while the specimen reacted against a four-arm bridge strain gauge load cell. A multichannel FM magnetic tape recorder and a multichannel transient recorder were used to store the test results. For the low-speed tests, load and displacement data were recorded directly to a Model 136A Hewlett-Packard recorder, but for the intermediate and high-speed tests, the data were stored in the digital memory of a transient recorder for playback at reduced speeds into the X-Y recorder. The FM tape recorder (Electro-Mechanical Research Inc., Sarasota, Florida, Model 392A) was used as a back-up recorder on the high-speed tests.

Circular cutouts in the loading heads of the test fixture were utilized to locate the potted specimens within the test fixture. A test fixture chamber was designed to contain each specimen during the tests while providing a steel and transparent plastic enclosure to be used for observing and photographing the test specimen.

DATA REDUCTION METHODOLOGY

A typical test curve is presented in Figure 3. The load on the test specimen is plotted on the ordinate versus ram displacement (specimen deformation) on the abscissa. The four dependent variables were extracted directly from the test curves and have units of load or deformation or combinations thereof. These variables are

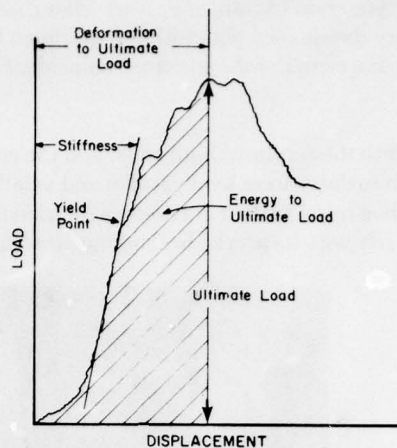


Figure 3. A Typical Load versus Displacement Test Curve.

ultimate load, deformation to ultimate load, stiffness, and energy to ultimate load. The first point on the load deformation curve, following the apparent elastic section, where the tangent to the curve becomes parallel to the deformation axis of the plot (abscissa), is defined as the ultimate load. The deformation to this point is defined as the deformation to ultimate load. The stiffness of the test specimen is determined by fitting the apparent linear elastic section of the load deformation curve with a least squares curve. The energy to ultimate is defined as the area under the load versus deformation test curve, from the point of zero deformation up to the deformation at ultimate load.

Three additional dependent variables were determined for each specimen. These variables are in units of engineering stress and strain and are, therefore, dependent upon the load-deformation and specimen geometry data. The ultimate engineering stress was computed from the ultimate load by dividing by the specimen area. The engineering strain as ultimate engineering stress was defined as the deformation to ultimate load divided by the original length of the test specimen. The test specimen elastic modulus was computed from the test specimen stiffness using the following relationship with typical units:

$$\text{Elastic Modulus (P}_a\text{)} = \text{Stiffness (N/m)} \frac{\text{Specimen Original Length (m)}}{\text{Specimen Area (m}^2\text{)}}$$

STATISTICAL ANALYSIS

A series of mechanical compression tests was conducted on fresh thoracic and lumbar vertebral centra excised from the Rhesus monkey [*Macaca mulatta*]. The purpose of the tests was to identify the effect of displacement rate and vertebral body position on mechanical strength. In total, twelve vertebral bodies were tested from each vertebral column; of these, five were thoracic and seven were lumbar.

The experimental design was influenced by several factors. Since the tests were destructive, different displacement rates could not be applied to the same test specimens. Since the vertebral bodies are associated with individual primates and vertebral body position is a factor of interest, the three displacement rates had to be applied to all positions in each primate to account for any variation among primates and among vertebral portions. In order to accommodate the six displacement rates, it was assumed that adjacent vertebrae would exhibit relatively minor variations in mechanical properties in comparison to the magnitude of the effects being sought. Accordingly, the twelve vertebral centra from each spinal column were grouped in sets of three, with each group representing a position. These groups were designated as P₁, P₂, P₃ and P₄; where P₁ represented vertebrae T₈, T₉, T₁₀; P₂ represented T₁₁, T₁₂, L₁; P₃ represented L₂, L₃, L₄; and P₄ represented L₅.

L₆ and L₇. With this assumption, each of the displacement rates could be applied to the subject-position combination. To the extent possible, the displacement rates were balanced across primate spinal column by assignments to particular vertebrae as seen in the following matrix.

The spinal columns were divided into two groups. Group I consisted of X96 (S₂), 884A (S₃), X90 (S₄), A104 (S₁). Group II consisted of W92 (S₈), 34A (S₅), 584 (S₆) and 882A (S₇). R₁, R₂, R₃, etc. corresponded to the various strain rates as shown below:

$$R_1 = 8.89 \times 10^{-6} \text{ meters per second}$$

$$R_2 = 8.89 \times 10^{-5} \text{ meters per second}$$

$$R_3 = 8.89 \times 10^{-4} \text{ meters per second}$$

$$R_4 = 8.89 \times 10^{-3} \text{ meters per second}$$

$$R_5 = 8.89 \times 10^{-2} \text{ meters per second}$$

$$R_6 = 8.89 \times 10^{-1} \text{ meters per second}$$

The test matrix is shown in Table 1. For Phase I the statistical model for this experiment is given by:

$$Y_{ijk} = \mu + S_i + P_{j(i)} + R_k + SR_{ik} + e_{ijk}$$

where

Y = mechanical properties of interest

μ = overall mean

S_i = differential effect due to subject i

P_{j(i)} = differential effect due to vertebral position j within subject i

R_k = differential effect due to displacement rate k

SR_{ik} = differential joint effect of subject i and displacement rate k

e_{ijk} = random error associated with measurement in subject i, position j, and displacement rate k

i = subject

j = spinal level

k = strain rate

The analysis of variance for the model is presented in Table 2.

TABLE 1
TEST MATRIX FOR VERTEBRAL BODY COMPRESSION TESTS (R = STRAIN RATE;
S = SUBJECT; P = SPINAL POSITION)

Subject	Rate	Position			
		P ₁	P ₂	P ₃	P ₄
Group I					
X96 (S ₂)	R ₁	T ₈	T ₁₁	L ₂	L ₅
	R ₂	T ₉	T ₁₂	L ₃	L ₆
	R ₃	T ₁₀	L ₁	L ₄	L ₇
884A (S ₃)	R ₁	T ₉	T ₁₂	L ₃	L ₆
	R ₂	T ₁₀	L ₁	L ₄	L ₇
	R ₃	T ₈	T ₁₁	L ₂	L ₅
X90 (S ₄)	R ₁	T ₁₀	L ₁	L ₄	L ₇
	R ₂	T ₈	T ₁₁	L ₂	L ₅
	R ₃	T ₉	T ₁₂	L ₃	L ₆
A104 (S ₁)	R ₁	T ₈	L ₁	L ₃	L ₅
	R ₂	T ₉	T ₁₁	L ₂	L ₇
	R ₃	T ₁₀	T ₁₂	L ₄	L ₆
Group II					
W92 (S ₈)	R ₄	T ₈	T ₁₁	L ₂	L ₅
	R ₅	T ₉	T ₁₂	L ₃	L ₆
	R ₆	T ₁₀	L ₁	L ₄	L ₇
34A (S ₅)	R ₄	T ₉	T ₁₂	L ₃	L ₆
	R ₅	T ₁₀	L ₁	L ₄	L ₇
	R ₆	T ₈	T ₁₁	L ₂	L ₅
584A (S ₆)	R ₄	T ₁₀	L ₁	L ₄	L ₇
	R ₅	T ₈	T ₁₁	L ₂	L ₅
	R ₆	T ₉	T ₁₂	L ₃	L ₆
882A	R ₄	T ₁₀	T ₁₂	L ₂	L ₅
	R ₅	T ₉	T ₁₁	L ₄	L ₆
	R ₆	T ₈	L ₁	L ₃	L ₇

TABLE 2

GENERAL ANALYSIS OF VARIANCE TABLE FOR VERTEBRAL BODY TESTING DATA

	Subject	Position (P)	Displacement Rate (R)	RP
Ult. Load	0.95	0.95	0.95	--
Deformation	0.95	0.95	0.95	--
Stiffness	--	0.90	0.95	--
Energy	0.95	0.95	--	--
Ult. Stress	0.95	--	0.95	--
Strain to Ult.	0.95	0.95	0.95	0.90
Elastic Mod	0.95	0.95	0.95	--

Due to the destructive nature of the tests, replication of the test was not possible, and a pure estimate of error variance was not obtainable. The analysis shown in the above table assumed that the interaction or joint effect of displacement rate at locations within subject was negligible, thus permitting this test to be used as the estimate of error variance. (The plausibility of the assumption was verified by the data of this experiment.) To calculate the mean squares of Table 3, the test specimens were considered as being random samples from a population where position and displacement rate were considered as fixed effects.

To test for a significant difference between differential effects of the independent variables in an analysis of variance, the test statistically defined by the appropriate F ratio of observed mean squares was calculated. Under the null hypothesis of no difference, the variance term (σ^2) in the expected mean squares of that effect is zero, and the expected F ratio is unity. Large F ratios calculated from observed data would indicate that the effect is present where the largeness can be determined for a given level of confidence from a table of critical F values. The critical F value was a function of the degrees of freedom in the numerator and the denominator of the F ratio. Note that for this experiment, the effects of subjects, positions and the subject-by-displacement-rate interaction were determined by making a ratio of their observed mean square with that of the error term. The displacement rate effect, however, was determined by making a ratio of its observed mean square with that of the subject by displacement rate interaction. Once degrees of freedom are analogous to sample size, it can be seen that a smaller sample size is available for testing for displacement rate effect than for testing the effect of the other sources of variation. Increasing the number of subjects would increase the sample size.

The experiment of Phase II was conducted similarly to that of Phase I. Vertebral centra from four different monkeys were subjected to compressive loading under three different displacement rates. The loading rates in this Phase were set at $R_1 = 8.9 \times 10^{-6}$ m/s, $R_3 = 8.9 \times 10^{-4}$ m/s, and $R_5 = 8.9 \times 10^{-2}$ m/s. The objective of this experiment was to demonstrate that the form of the model derived in Phase I would apply to other displacement rates and to provide a larger sample size for estimating the parameters of the model.

The results from one of the test subjects W92 (Sg) was significantly different from the other seven subjects tested and as a result were not included in this analysis.

The regression analysis of the Phase I data indicated that an appropriate model for predicting any of the mechanical responses in Phase II has the form:

$$Y_{ij} = a_{p_i} + bx + e_{ij}$$

where

Y_{ij} = j^{th} response in position grouping i

a_{pi} = intercept for position grouping i

x = \log_{10} of displacement rate

b = response slope

e_{ij} = random error

Note that the qualitative variable of vertebral position is modeled by generating equations for different positions. The Phase I statistical analysis indicated that the effect due to position was not significant; therefore, only a single equation was derived for positions within the vertebral column. Similarly, when subgroupings of position displayed significant differences between subgroups but the difference within a subgrouping was not significant, a different constant was calculated for each subgroup.

TABLE 3

**PHASE I – ULTIMATE LOAD (N)
AND ANALYSIS OF VARIANCE TABLE**

		P ₁	P ₂	P ₃	P ₄
R ₂	S ₁	2447	4092	4849	5516
	S ₂	2113	2936	4048	4448
	S ₃	2157	3292	4715	5204
	S ₄	2068	2580	2936	3203
R ₄	S ₁	3336	3870	5783	6494
	S ₂	2891	4893	4671	5694
	S ₃	3190*	4444	5738	6583
	S ₄	2091	2313	3205	4003
R ₆	S ₁	4448	5961	7206	8096
	S ₂	3692	6032	5516	8452
	S ₃	2936	4003	6672	8185
	S ₄	2802	3718*	4359	5738

*Estimated value of missing data point.

Analysis of Variance Table

Source of Variation	Degrees of Freedom	Mean Square	F Ratio	Level of Confidence
S	3	8.478×10^6	23.24	0.95
R	3	15.438×10^6	42.26	0.95
P	2	21.298×10^6	58.31	0.95
RP	6	0.612×10^6	1.67	---
Error	31	0.365×10^6		

The ultimate loads for Phase II are shown in Table 4. The effects due to both displacement rate and vertebral body position were also found to be significant. The ultimate load for R₅ was greater than R₃, which was in turn greater than R₁.

TABLE 4
PHASE II RESULTS – ULTIMATE LOADS (N)

		P ₁	P ₂	P ₃	P ₄
R ₁	S ₅	2157	2713	3781	3781
	S ₆	2269	2758	3136	3247
	S ₇	2891	3514	3781	5471
	S ₈	867	1090	1601	1668
R ₃	S ₅	2891	3737	4537	4671
	S ₆	2313	2713	3781	4181
	S ₇	4300	3914	5605	6939
	S ₈	1223	1334	2535	1824
R ₅	S ₅	1935	3648	5071	5204
	S ₆	2580	3959	5115	5560
	S ₇	4212	5783	6850	8007
	S ₈	1646	1913	2269	2402

RESULTS AND DISCUSSIONS

The values of the mechanical properties that were reduced from the test data are given in Appendix I and Appendix II.

ULTIMATE LOAD

The ultimate loads along with the calculated analysis of variance are shown in Table 3. The effects due to both displacement rate and vertebral position were found to be significant. In particular, the average ultimate load for R₆ was significantly greater than that for R₄, which in turn was significantly greater than the average ultimate load for R₂. Similarly, the average ultimate loads for the four positions were all significantly different with $P_4 > P_3 > P_2 > P_1$. Figure 4 identifies average load as a function of displacement rate for each position. The results indicate that ultimate load is a linear function of log displacement rates, with different constants being a function of vertebral level or position.

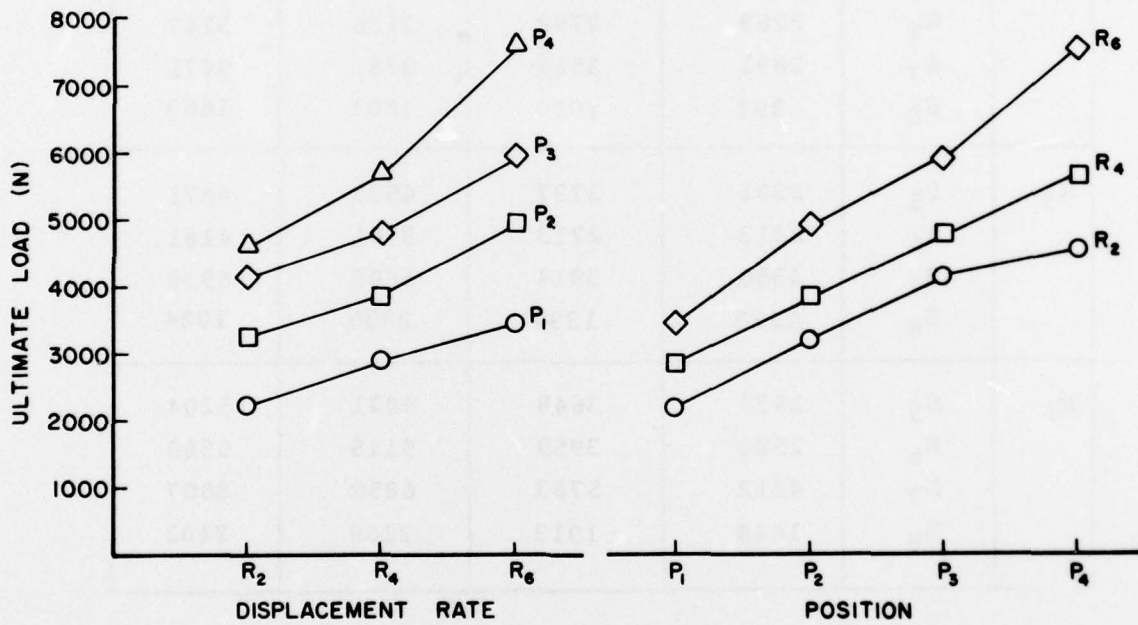


Figure 4. Average Ultimate Load for Position by Displacement Rate Combinations.

DEFORMATION TO ULTIMATE LOAD

The values of deformation to ultimate load observed during Phase I and their analysis of variance summary are presented in Table 5. The effects due to displacement rate and position were significant. The average deformation for R₆ was significantly greater than that of R₄, which in turn was significantly greater than that of R₂. The average deformation for P₁ was significantly less than the other three, and that of P₄ was significantly greater than the others. No significant difference was noted between P₂ and P₃. The results shown in Figure 5 represent the average deformation for combination of position and displacement rate. The linear change of deformation with log displacement rate is not as clearly defined as in the ultimate load values. The data show considerably more scatter.

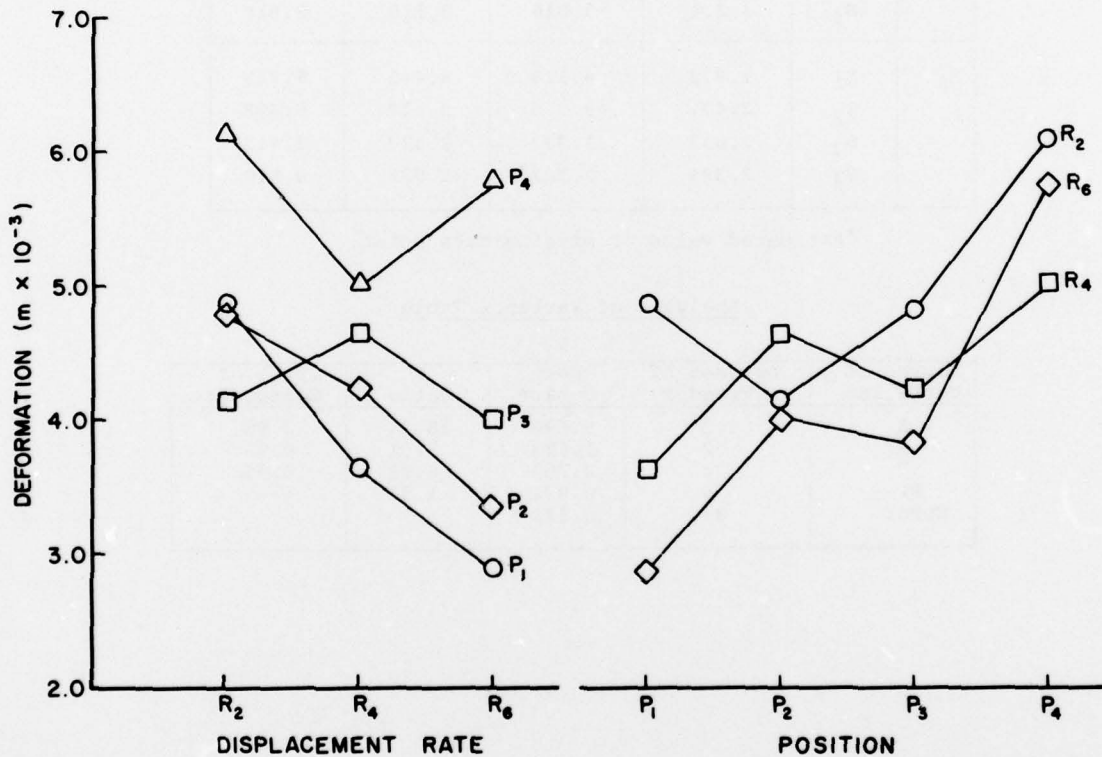


Figure 5. Average Deformation to Ultimate Load for Position by Displacement Rate Combinations.

TABLE 5

PHASE I RESULTS – DEFORMATION TO ULTIMATE LOAD ($m \times 10^{-3}$)

		P ₁	P ₂	P ₃	P ₄
R ₂	S ₁	4.890	4.648	5.080	6.096
	S ₂	2.699	2.540	3.937	4.318
	S ₃	2.540	2.350	2.667	3.175
	S ₄	4.445	2.883	2.667	4.763
R ₄	S ₁	4.763	4.604	4.445	5.080
	S ₂	3.016	3.366	2.223	2.667
	S ₃	1.868*	2.985	2.223	3.493
	S ₄	1.270	3.016	3.810	3.810
R ₆	S ₁	1.778	4.128	4.445	5.715
	S ₂	2.477	3.175	2.527	5.398
	S ₃	2.032	1.937	2.527	2.413
	S ₄	2.381	2.767*	2.032	3.810

*Estimated value of missing data point.

Analysis of Variance Table

Source of Variation	Degrees of Freedom	Mean Square	F Ratio	Level of Confidence
S	3	9.690	18.94	0.95
R	2	1.693	3.31	0.95
P	3	4.253	8.31	0.95
RP	6	0.671	1.31	---
Error	31	0.512		

The Phase II results with respect to deformation to ultimate load are similar to that of the above; the average deformation for R₅ was significantly greater than that of R₃, which in turn was conclusively above that of R₁. These results are shown in Table 6.

TABLE 6
PHASE II RESULTS – DEFORMATION TO ULTIMATE LOAD (m x 10⁻³)

		P ₁	P ₂	P ₃	P ₄
R ₁	S ₅	5.080	4.763	6.350	6.223
	S ₆	1.778	2.159	3.810	8.128
	S ₇	4.445	5.080	3.366	6.985
	S ₈	2.159	2.540	4.572	1.778
R ₃	S ₅	5.398	4.763	8.255	6.668
	S ₆	2.096	2.858	3.493	4.445
	S ₇	---	3.175	5.715	5.906
	S ₈	2.191	3.239	4.445	1.905
R ₅	S ₅	1.429	4.604	5.715	4.572
	S ₆	1.588	2.699	3.493	5.080
	S ₇	---	5.080	3.937	5.080
	S ₈	3.651	2.858	1.969	1.588

STIFFNESS

The stiffness values and their analysis of variance are shown in Table 7. Displacement rate was significant with higher rates of loading resulting in larger stiffness values. The position effect was significant at the 90 percent confidence level, however not at the 95 percent level of confidence. Since the means for P₁ and P₂ (2.62 and 2.81 N/m² x 10⁶, respectively) were approximately equal, separate regression models were derived for each of the two position groupings. The results are presented in Figure 6, which provides average stiffness for combinations of displacement rates and position. The response of stiffness due to the controlled factors is not always consistent for the individual position grouping or displacement rates, but the significant trends can be discerned. A similar trend was noted to be present in the Phase II stiffness data shown in Table 8.

TABLE 7
PHASE I RESULTS – STIFFNESS (N/m x 10⁶)

		P ₁	P ₂	P ₃	P ₄
R ₂	S ₁	1.067	1.879	1.728	2.179
	S ₂	0.885	1.492	1.788	1.230
	S ₃	1.023	1.804	2.257	2.058
	S ₄	6.273	1.057	1.696	1.584
R ₄	S ₁	1.268	1.463	3.395	3.152
	S ₂	1.226	1.783	4.041	4.028
	S ₃	1.809*	1.611	3.573	3.065
	S ₄	2.038	0.866	1.051	2.335
R ₆	S ₁	2.709	3.379	3.940	2.335
	S ₂	1.121	2.001	5.004	3.713
	S ₃	1.821	4.641	3.244	5.511
	S ₄	2.371	3.337*	3.503	3.585

*Estimated value of missing data point.

Analysis of Variance Table

Source of Variation	Degrees of Freedom	Mean Square	F Ratio	Level of Confidence
S	3	0.448	0.34	---
R	3	8.115	6.15	0.95
P	2	3.126	2.37	0.90
RP	6	1.831	1.39	---
Error	31	1.319		

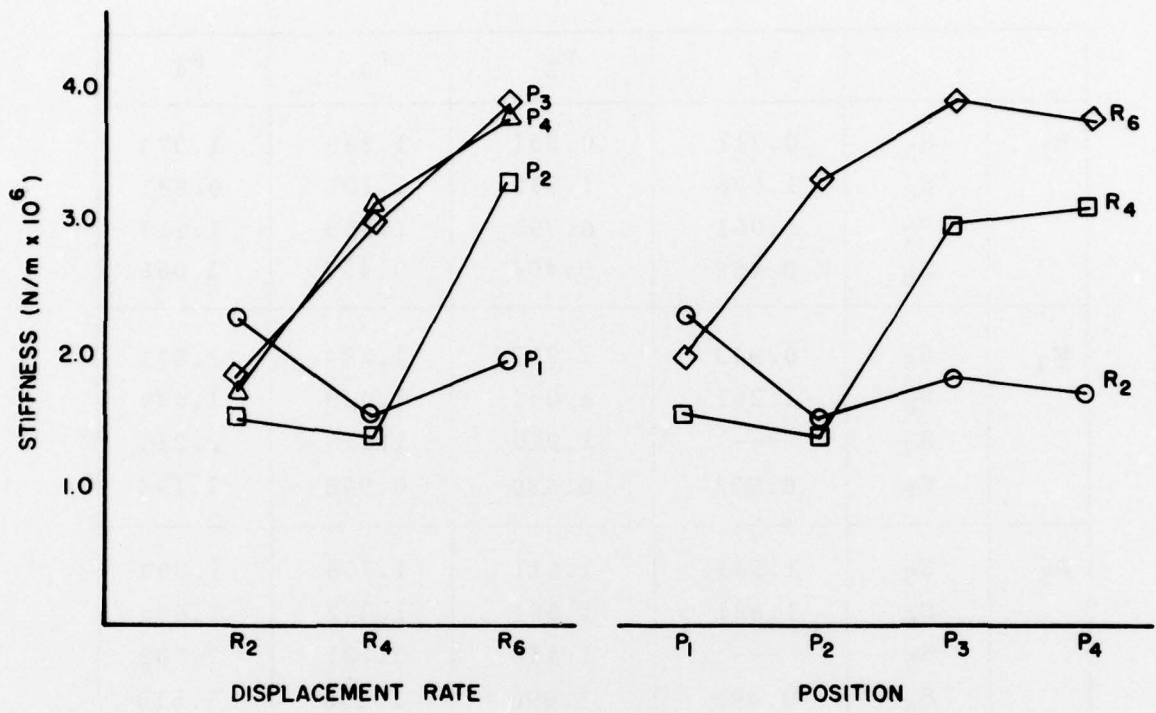


Figure 6. Stiffness for Position by Displacement Rate Combinations.

TABLE 8
PHASE II RESULTS – STIFFNESS (N/m x 10⁶)

		P ₁	P ₂	P ₃	P ₄
R ₁	S ₅	0.711	0.861	1.868	1.373
	S ₆	1.576	1.560	1.101	0.881
	S ₇	1.061	0.799	1.653	1.217
	S ₈	0.458	0.494	0.457	1.066
R ₃	S ₅	0.943	1.907	1.284	1.541
	S ₆	1.261	1.051	1.423	1.479
	S ₇	---	1.910	1.615	2.215
	S ₈	0.631	0.480	0.978	1.194
R ₅	S ₅	1.541	1.611	1.706	1.500
	S ₆	1.821	1.681	1.842	1.691
	S ₇	---	1.416	3.121	2.802
	S ₈	0.490	1.090	1.168	1.518

ENERGY TO ULTIMATE LOAD

The values of energy to ultimate load obtained during the Phase I tests are shown in Table 9 along with the analysis of variance summary. The effect due to displacement rate was not significant, but the effect due to vertebral centrum position within the spinal column was significant. These results are discernible from Figure 7, which presents average energy for combination of displacement rate at position. Like results are noted in the Phase II energy to ultimate load data shown in Table 10.

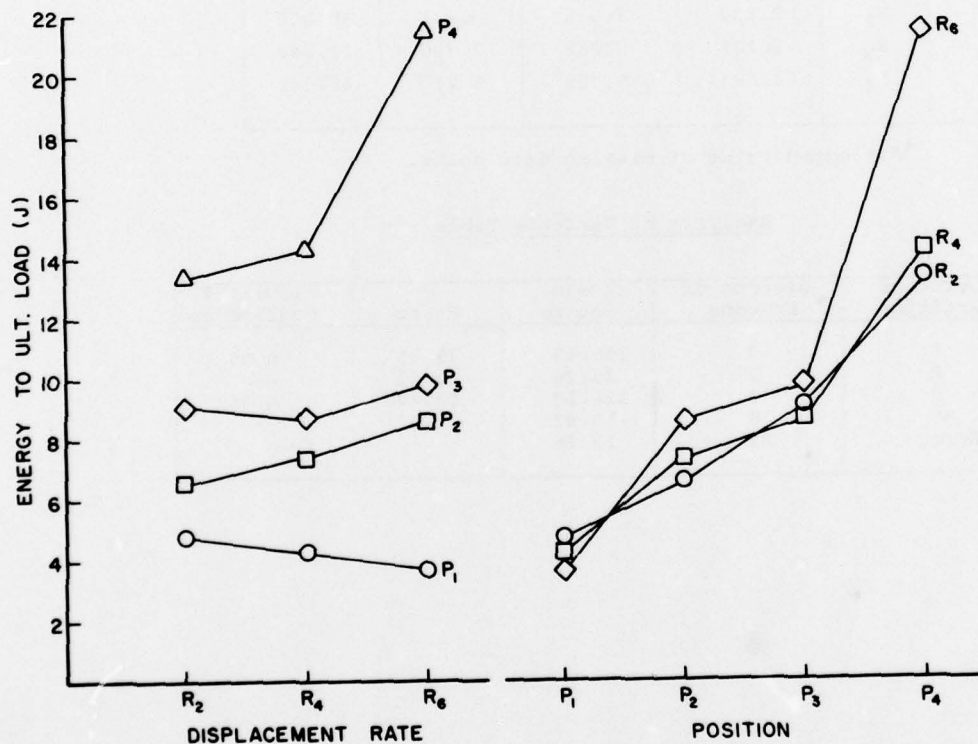


Figure 7. Average Energy to Ultimate Load for Position by Displacement Rate Combinations.

TABLE 9

PHASE I RESULTS – ENERGY TO ULTIMATE LOAD (J)

		P ₁	P ₂	P ₃	P ₄
R ₂	S ₁	7.987	14.259	16.456	24.049
	S ₂	2.881	3.994	3.717	9.869
	S ₃	2.870	4.429	6.463	8.920
	S ₄	5.357	3.850	4.678	10.739
R ₄	S ₁	9.736	10.996	18.241	21.942
	S ₂	4.316	9.276	6.999	10.344
	S ₃	1.629*	6.022	7.338	14.349
	S ₄	1.370	3.265	2.146	10.434
R ₆	S ₁	3.305	16.597	22.134	27.580
	S ₂	3.839	7.355	3.921	30.834
	S ₃	3.101	5.268	7.380	12.248
	S ₄	4.384	5.308*	5.259	15.389

*Estimated value of missing data point.

Analysis of Variance Table

Source of Variation	Degrees of Freedom	Mean Square	F Ratio	Level of Confidence
S	3	386.67	29.15	0.95
R	2	29.26	2.21	---
P	3	316.18	23.84	0.95
RP	6	18.92	1.43	---
Error	31	13.26		

TABLE 10

PHASE II RESULTS — ENERGY TO ULTIMATE LOAD (J)

		P ₁	P ₂	P ₃	P ₄
R ₁	S ₅	6.799	7.819	17.451	16.468
	S ₆	2.642	2.949	6.672	10.214
	S ₇	7.453	7.666	7.700	22.563
	S ₈	0.859	1.408	4.000	1.347
R ₃	S ₅	9.827	12.835	25.970	21.173
	S ₆	2.583	3.632	6.728	11.988
	S ₇	---	7.604	19.315	26.269
	S ₈	1.637	2.110	7.355	1.638
R ₅	S ₅	1.212	11.462	18.959	12.530
	S ₆	1.840	4.638	9.756	16.965
	S ₇	---	17.982	16.383	25.681
	S ₈	2.781	3.197	1.667	1.678

ULTIMATE ENGINEERING STRESS

The values of ultimate engineering stress and their analysis of variance summary are presented in Table 11. The effect of displacement rate is significant with higher values of ultimate stress resulting from the faster displacement rates. The position effect, however, was not significant. These results can be seen in Figure 8, which presents average ultimate stress for combinations of displacement rate and position. Phase II results are presented in Table 12. The results are similar to the above findings.

TABLE 11

PHASE I RESULTS — ULTIMATE ENGINEERING STRESS (Pa x 10⁶)

		P ₁	P ₂	P ₃	P ₄
R ₂	S ₁	19.056	19.049	19.987	21.644
	S ₂	14.621	14.220	15.454	15.494
	S ₃	14.995	18.621	18.456	17.966
	S ₄	11.963	9.874	9.230	10.257
R ₄	S ₁	21.457	21.577	25.177	23.410
	S ₂	17.998	19.497	17.237	18.048
	S ₃	22.300*	21.465	22.517	21.437
	S ₄	15.579	10.545	11.750	12.215
R ₆	S ₁	21.669	29.707	29.163	30.756
	S ₂	20.810	22.638	23.686	25.486
	S ₃	26.768	26.294	29.133	29.850
	S ₄	18.405	17.876*	14.531	16.941

*Estimated value of missing data point.

Analysis of Variance Table

Source of Variation	Degrees of Freedom	Mean Square	F Ratio	Level of Confidence
S	3	259.07	75.24	0.95
R	2	280.41	81.44	0.95
P	3	5.67	1.65	---
RP	6	3.56	1.03	---
Error	31	3.44		

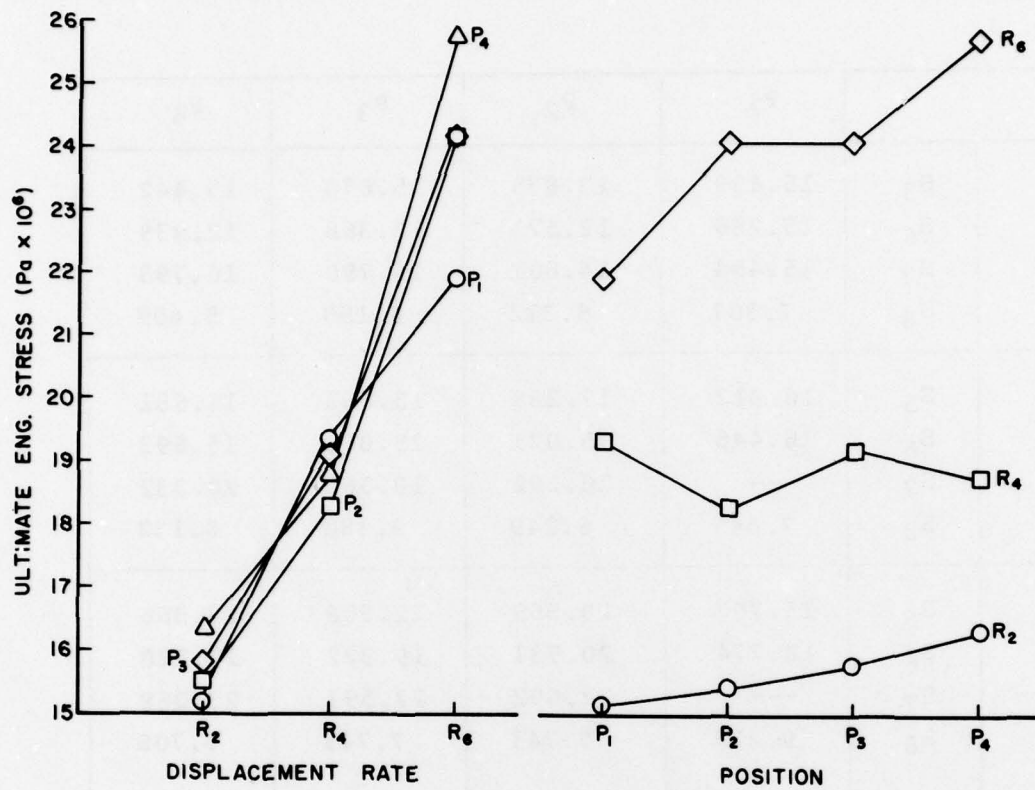


Figure 8. Average Ultimate Engineering Stress for Position by Displacement Rate Combinations.

TABLE 12

PHASE II RESULTS – ULTIMATE ENGINEERING STRESS (Pa x 10⁶)

		P ₁	P ₂	P ₃	P ₄
R ₁	S ₅	15.699	13.835	15.670	13.442
	S ₆	15.288	12.573	12.368	12.939
	S ₇	15.454	14.801	13.790	16.793
	S ₈	7.307	5.312	6.159	5.409
R ₃	S ₅	16.912	17.288	15.663	16.681
	S ₆	16.446	15.021	15.066	15.693
	S ₇	---	20.292	18.061	20.332
	S ₈	7.645	6.249	9.380	6.132
R ₅	S ₅	15.703	20.559	21.358	17.966
	S ₆	18.774	20.731	19.922	20.520
	S ₇	---	22.692	22.591	23.068
	S ₈	9.277	7.741	7.745	7.708

ENGINEERING STRAIN TO ULTIMATE STRESS

The strain values obtained during the Phase I tests are presented in Table 13 along with their analysis of variance. The displacement rate and position effects are significant at the 95% level of confidence, while the joint effect of displacement rate at position is significant at the 90% level of confidence. Since this is the only response for which the interaction is significant and since it is not significant at a high level of confidence, the interaction term was removed in modeling the strain response as a function of displacement rate at position. The average strain measurements did not display a consistent pattern; this is shown in Figure 9. There is a decreasing average strain for increasing displacement rate and a trend toward lower strains for P₃ and P₄ than for P₁ and P₂. As a result, strain was modeled in terms of log displacement rate with P₁ and P₂ in one subgrouping and P₃ and P₄ in a record subgrouping. Phase II results as shown in Table 14 reflected similar findings.

TABLE 13

PHASE I RESULTS – ENGINEERING STRAIN TO ULTIMATE STRESS (m/m)

		P ₁	P ₂	P ₃	P ₄
R ₂	S ₁	0.507	0.306	0.294	0.302
	S ₂	0.280	0.182	0.211	0.199
	S ₃	0.265	0.182	0.145	0.144
	S ₄	0.378	0.185	0.132	0.243
R ₄	S ₁	0.469	0.376	0.266	0.300
	S ₂	0.282	0.228	0.110	0.124
	S ₃	0.229*	0.203	0.111	0.168
	S ₄	0.130	0.238	0.206	0.179
R ₆	S ₁	0.161	0.308	0.232	0.293
	S ₂	0.191	0.191	0.122	0.269
	S ₃	0.218	0.159	0.153	0.112
	S ₄	0.233	0.188*	0.104	0.176

*Estimated value of missing data point.

Analysis of Variance Table

Source of Variation	Degrees of Freedom	Mean Square	F Ratio	Level of Confidence
S	3	0.05007	17.48	0.95
R	2	0.01131	3.95	0.95
P	3	0.02294	8.01	0.95
RP	6	0.00638	2.23	0.90
Error	31	0.00286		

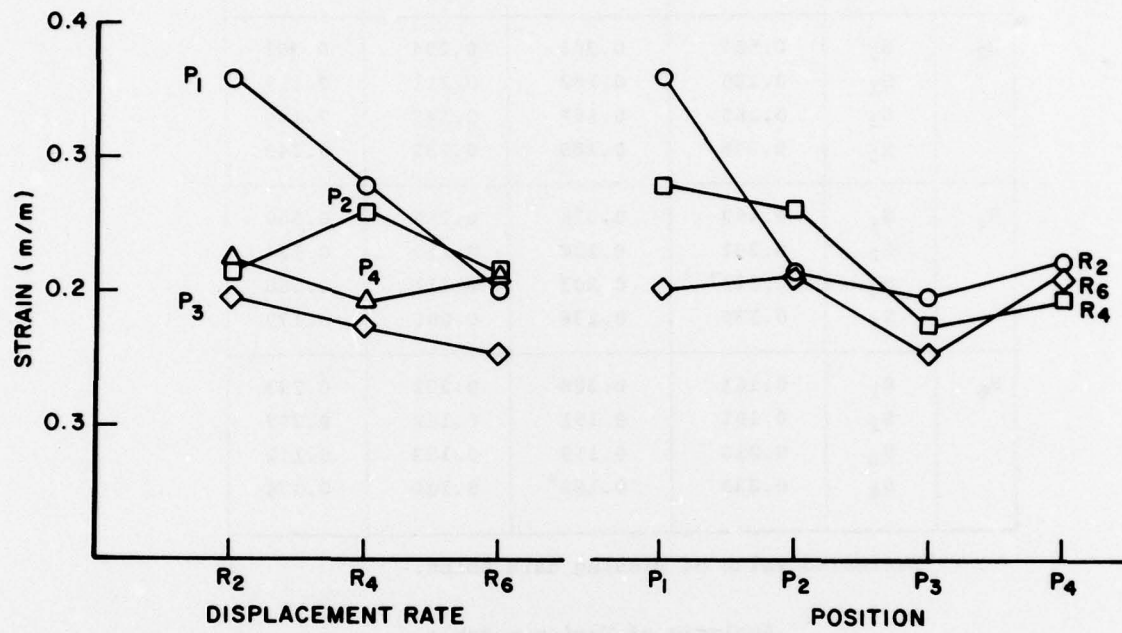


Figure 9. Average Engineering Strain to Ultimate for Position by Displacement Rate Combinations.

TABLE 14

PHASE II RESULTS – ENGINEERING STRAIN TO ULTIMATE STRESS (m/m)

		P ₁	P ₂	P ₃	P ₄
R ₁	S ₅	0.464	0.290	0.303	0.274
	S ₆	0.146	0.131	0.186	0.453
	S ₇	0.361	0.327	0.177	0.304
	S ₈	0.228	0.210	0.259	0.087
R ₃	S ₅	0.423	0.262	0.382	0.406
	S ₆	0.212	0.213	0.193	0.203
	S ₇	---	0.231	0.269	0.266
	S ₈	0.222	0.228	0.239	0.091
R ₅	S ₅	0.140	0.320	0.307	0.187
	S ₆	0.150	0.182	0.182	0.246
	S ₇	---	0.290	0.193	0.262
	S ₈	0.351	0.185	0.095	0.082

ELASTIC MODULUS

The Phase I values of elastic modulus and their analysis of variance are presented in Table 15. Both the displacement rates and position effects are significant. The elastic modulus increases with increasing displacement rate as is apparent from Figure 10. The increase is approximately linear with log displacement rate. The average elastic modulus for P₁ is significantly less than that of P₂, which in turn is significantly less than that of P₃ and P₄. The differences in average elastic modulus between P₃ and P₄ is not significant. These trends are readily observable in Figure 10 and are also similar as noted in Table 16, which presents Phase II results.

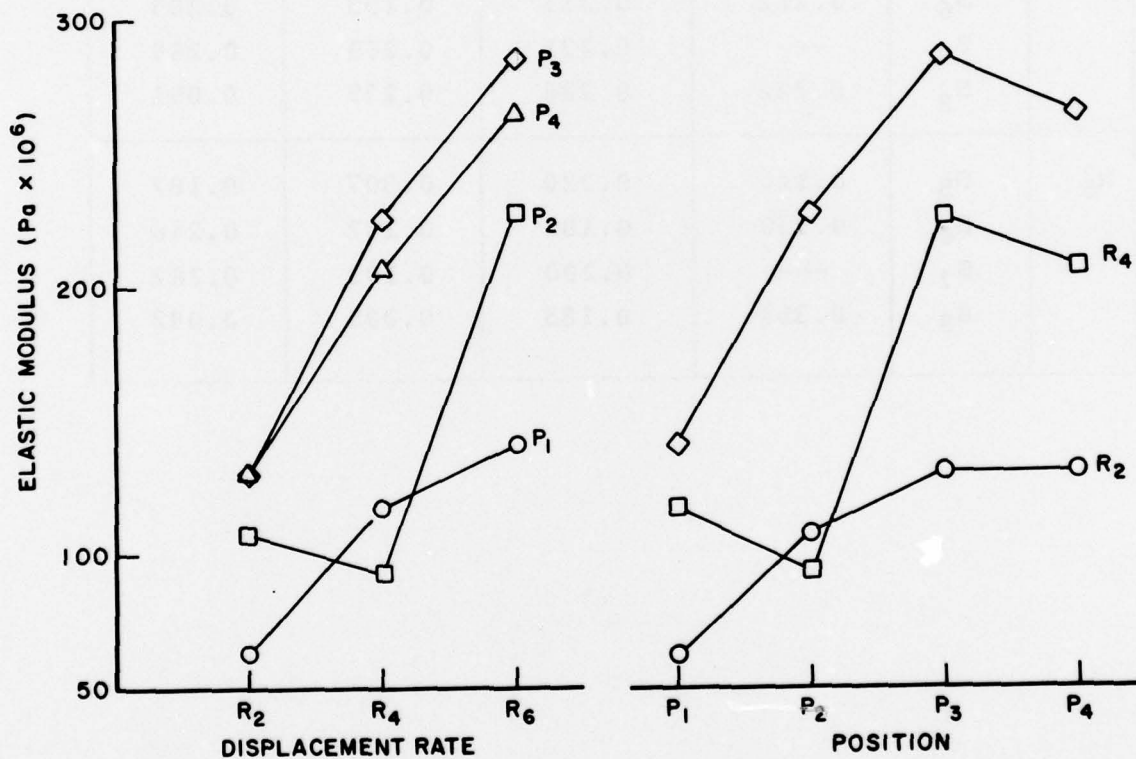


Figure 10. Average Elastic Modulus for Position by Displacement Rate Combinations.

TABLE 15
PHASE I RESULTS — ELASTIC MODULUS (Pa x 10⁶)

		P ₁	P ₂	P ₃	P ₄
R ₂	S ₁	80.2	133.1	123.2	172.7
	S ₂	58.9	100.6	127.1	93.1
	S ₃	68.3	132.0	162.9	156.9
	S ₄	42.7	63.2	107.8	99.3
R ₄	S ₁	82.8	99.9	247.5	192.4
	S ₂	81.6	104.8	300.3	274.8
	S ₃	157.1*	115.7	279.9	207.1
	S ₄	148.1	50.0	75.5	151.9
R ₆	S ₁	188.9	225.8	305.7	172.8
	S ₂	82.0	125.0	377.3	224.6
	S ₃	154.4	370.4	233.8	429.3
	S ₄	138.1	188.3*	228.3	229.0

*Estimated value of missing data point.

Analysis of Variance Table

Source of Variation	Degrees of Freedom	Mean Square	F Ratio	Level of Confidence
S	3	12498	3.47	0.95
R	2	59861	16.63	0.95
P	3	30158	8.38	0.95
RP	6	3717	1.03	---
Error	31	3599		

TABLE 16
PHASE II RESULTS — ELASTIC MODULUS (Pa x 10⁶)

		P ₁	P ₂	P ₃	P ₄
R ₁	S ₅	56.7	72.0	162.4	111.0
	S ₆	129.0	117.6	89.1	62.9
	S ₇	69.9	52.3	114.8	85.8
	S ₈	36.4	29.2	31.1	70.4
R ₃	S ₅	70.3	160.3	108.8	90.5
	S ₆	88.8	78.2	102.9	121.4
	S ₇	---	135.8	210.2	147.5
	S ₈	38.9	32.0	67.1	83.6
R ₅	S ₅	128.0	130.6	133.5	128.4
	S ₆	140.4	130.8	137.9	128.8
	S ₇	---	97.3	110.4	156.7
	S ₈	28.8	68.3	89.9	94.3

The mechanical property responses of interest just described were: ultimate load, deformation to ultimate load, stiffness, energy to ultimate load, ultimate engineering stress, engineering strain to ultimate stress, and elastic modulus. For each of these dependent variables, an analysis of variance was performed on the resulting measurements. Table 17 summarizes the results of these analyses. Since variation between monkeys was expected, this source of variation was isolated in the analyses to provide better discrimination among the levels of the other factors. A significant effect for subject (monkeys) indicates that differences in response were observed for the monkeys, but this observation has no other practical significance.

TABLE 17

SUMMARY OF REGRESSION RESULTS FOR RHESUS MONKEYS

Physical Property	R	S(e)	Slope (b)	Position Grouping	a_{p_i}
Ultimate Load (N)	0.83	936	448	P ₁ P ₂ P ₃ P ₄	3014 4230 5132 5965
Deformation (m x 10 ⁻³)	0.55	1.317	-0.271	P ₁ P ₂ , P ₃ P ₄	2.796 3.533 4.754
Stiffness (N/m x 10 ⁶)	0.56	1.953	0.320	P ₁ , P ₂ P ₃ , P ₄	1.978 2.613
Energy (J)	0.65	5.64	0.399	P ₁ P ₂ P ₃ P ₄	4.836 8.424 11.667 17.449
Ultimate Eng. Stress (Pa x 10 ⁶)	0.68	3.657	1.911	P ₁ , P ₂ , P ₃ , P ₄	19.911
Strain (m/m)	0.41	0.086	-0.0159	P ₁ , P ₂ P ₃ , P ₄	0.247 0.212
Elastic Modulus	0.68	58.5	24.7	P ₁ P ₂ P ₃ , P ₄	119.6 145.1 188.2

The entries in Table 17 represent the level of confidence of rejecting the hypothesis of no effect due to the factor. Levels of confidence greater than 0.95 were not considered. Levels of confidence as low as 0.90 were reported since consistent trends were noted in the data and the large degree of scatter could prevent the trends from being statistically significant at a higher level of confidence. The absence of an entry indicates the effect is not significant at the 90% level of confidence.

THE REGRESSION MODEL

The qualitative variable of vertebral position is modeled by generating equations for different positions. However, when the Phase I analysis indicated that the effect due to position was not significant, only one equation was derived for all positions. Similarly, when subgroupings of position displayed significant differences between subgroups but the differences within a subgroup were not significant, a different constant was calculated for each subgroup.

The above model was fit to the combined data sets of Phase I and II, and the results are summarized in Table 17. For each of the physical properties, the table contains a single value for the correlation coefficient, the standard error, and the slope (coefficient of log displacement rate). The groupings of vertebral position are also indicated along with the intercept for each group. The percentage of total variation of the response mechanical properties explained by regression (r^2) varied from a high of 69% for ultimate load down to a low of 17% for engineering strain to ultimate stress. Thus, although the regression equations do provide a significant correlation with the measured mechanical properties, considerable unexplained variability due to uncontrolled and/or unmeasured factors still exists.

Figures 11 through 17 display the regression results for the first listed position grouping of Table 17. Load, deformation, energy, and elastic modulus are presented for P₁ (vertebral bodies T₈, T₉ and T₁₀). Stiffness and strain are presented for P₁ and P₂ (vertebral bodies T₈, T₉, T₁₀, T₁₁, T₁₂ and L₁) since no significant difference in these responses was detected for these position groupings. The figure for stress (Figure 11) is applicable to all positions since this factor did not significantly influence the ultimate stress determinations. Since the only difference between the regression equations for different positions is an additive constant, the presented curves are representative of all positions.

The five curves in each of these figures are estimates of percentiles of the individual responses at a particular displacement. That is, 25% of the response values from individual vertebrae would be expected to fall below the 25th percentile line. Further, 90% of individual responses would fall between the 5th and 95th percentile lines. These percentile lines (or others if desired) are based on the assumption of the random errors (e_{ij}) being normally distributed with equal variance for all displacement rates and can be generated from the data of Table 17.

Figures 11 through 17 also present the individual observed test values after correcting for applicable position effects. The correction is an additive constant equal to the difference in a_{pi} values from Table 17. Two conclusions can be drawn from an examination of the plots of the data. First, the two phases of the experiment resulted in a consistent relationship between the response properties over the range of displacement rates. The results of the two phases were in agreement. Second, the statistical assumptions required for the regression analysis are not grossly violated, and the percentile lines contain approximately the correct percentages of data points.

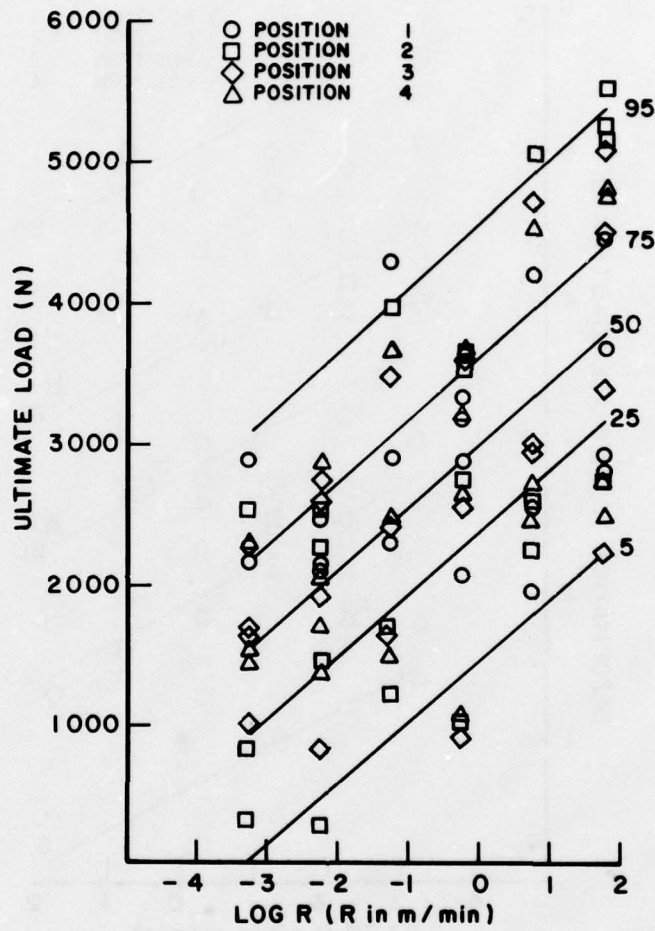


Figure 11. Regression Results for Stress vs. Displacement Rate — P1.

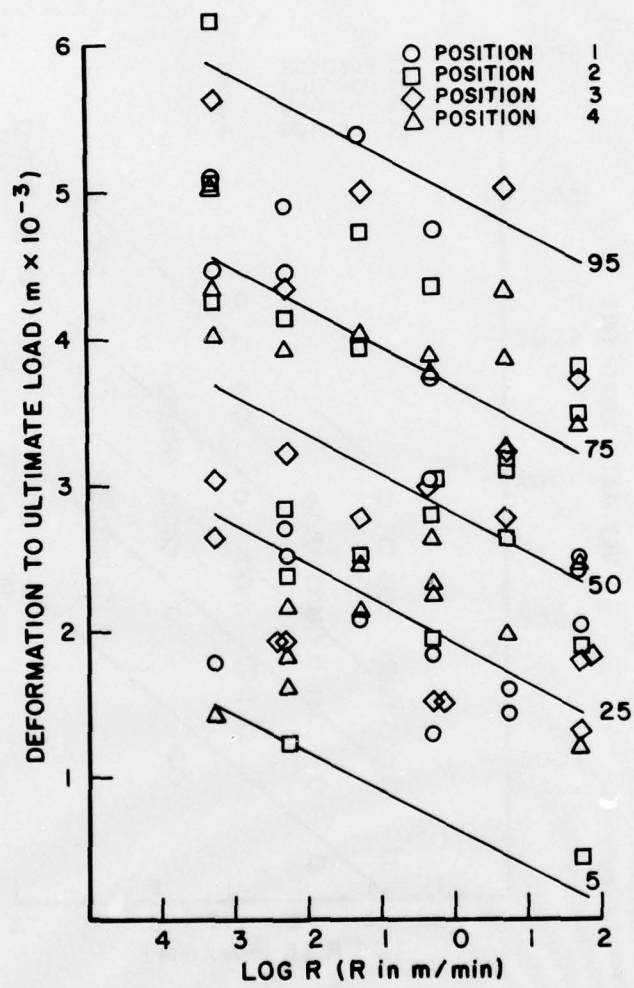


Figure 12. Regression Results for Deformation vs. Displacement Rate — P1.

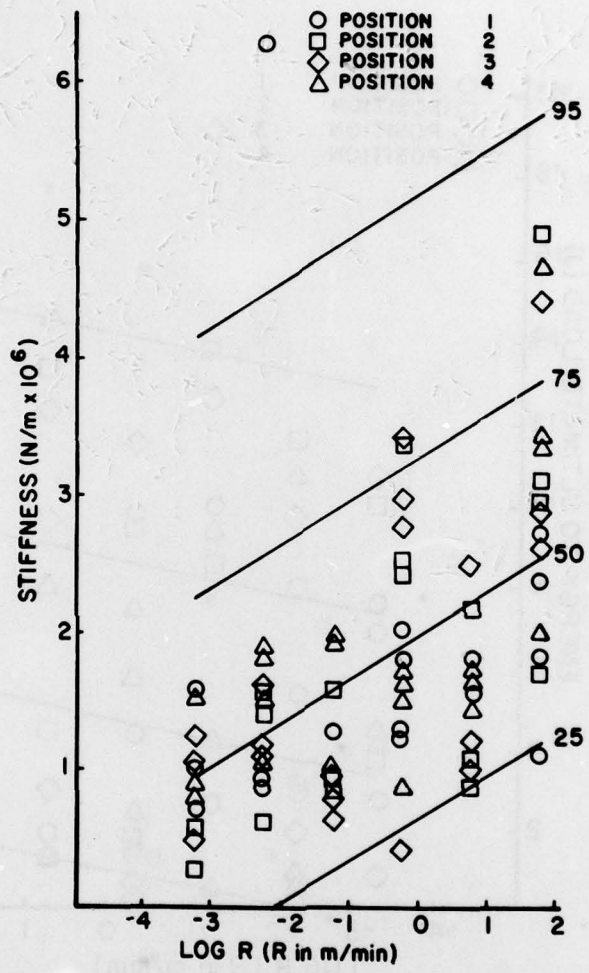


Figure 13. Regression Results for Stiffness vs. Displacement Rate — (P1 and P2).

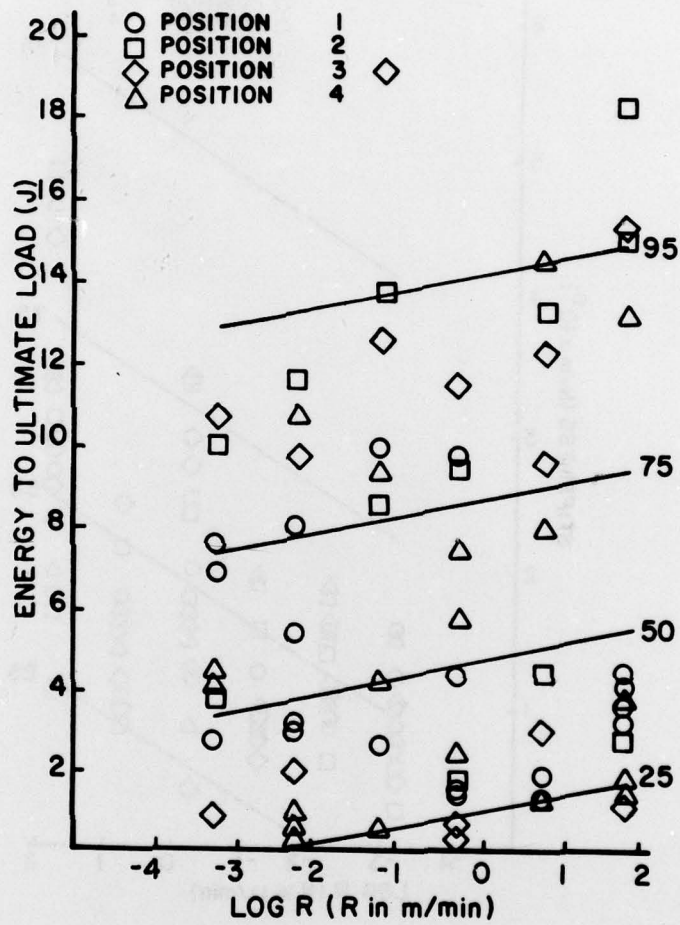


Figure 14. Regression Results for Energy vs. Displacement Rate — P1.

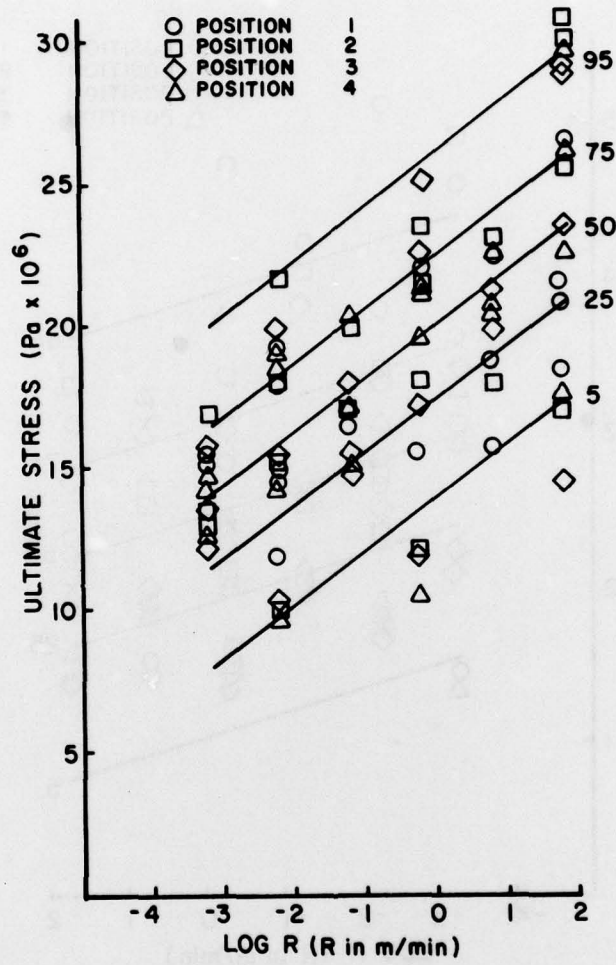


Figure 15. Regression Results for Stress vs. Displacement Rate — All positions.

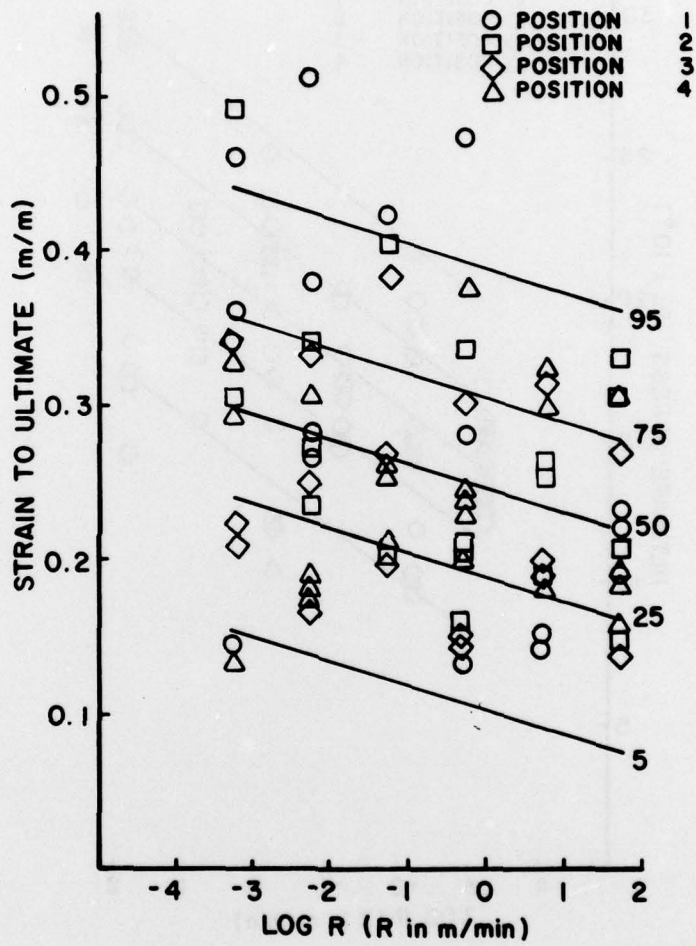


Figure 16. Regression Results for Strain vs. Displacement Rate — P1 and P2.

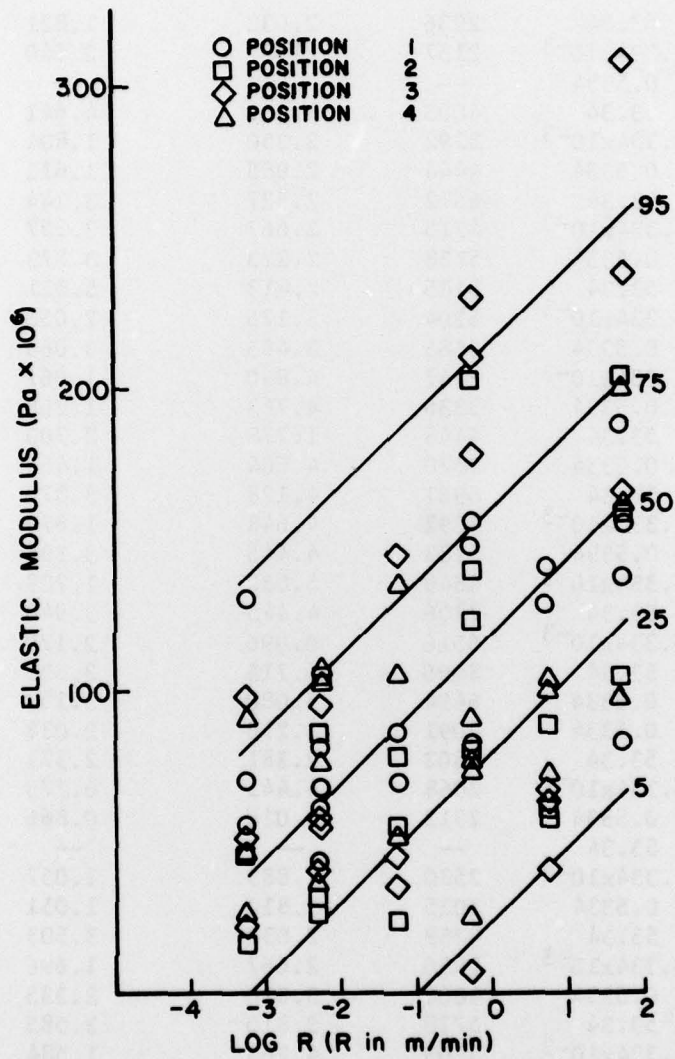


Figure 17. Regression Results for Elastic Modulus vs. Displacement Rate — P1.

APPENDIX I
ENGINEERING DATA OBTAINED FROM RHESUS
MONKEY SINGLE VERTEBRAL BODIES

Speciman No.	VB No.	Displace. Rate (m/min)	Ult. Load (N)	Def. to Ult. Load (Mx10 ⁻³)	Stiffness (N/mx10 ⁶)	Energy to Ult. Load (J)	
884A	T8	184	53.34	2936	2.032	1.821	3.101
884A	T9	185	5.334x10 ⁻³	2157	2157	2.540	2.870
884A	T10	186	0.5334	--	--	--	--
884A	T11	187	53.34	4003	1.937	4.641	5.268
884A	T12	188	5.334x10 ⁻³	3292	2.350	1.804	4.429
884A	L1	189	0.5334	4444	2.985	1.611	6.022
884A	L2	190	53.34	6672	2.527	3.244	7.830
884A	L3	191	5.334x10 ⁻³	4715	2.667	2.257	6.463
884A	L4	192	0.5334	5738	2.223	3.573	7.338
884A	L5	193	53.34	8185	2.413	5.511	12.248
884A	L6	194	5.334x10 ⁻³	5204	3.175	2.058	8.920
884A	L7	195	0.5334	6583	3.493	3.065	14.349
A104	T8	196	5.334x10 ⁻³	2447	4.890	1.067	7.987
A104	T9	197	0.5334	3336	4.763	1.268	9.736
A104	T10	198	53.34	4448	1.778	2.709	3.305
A104	T11	199	0.5334	3870	4.604	1.463	10.996
A104	T12	200	53.34	5961	4.128	3.379	16.597
A104	L1	201	5.334x10 ⁻³	4092	4.648	1.879	14.259
A104	L2	202	0.5334	5783	4.445	3.395	18.241
A104	L3	203	5.334x10 ⁻³	4849	5.080	1.728	16.456
A104	L4	204	53.34	7206	4.445	3.940	22.134
A104	L5	205	5.334x10 ⁻³	5516	6.096	2.179	24.049
A104	L6	206	53.34	8096	5.715	2.335	27.580
A104	L7	207	0.5334	6494	5.080	3.152	21.942
X90	T8	208	0.5334	2091	1.270	2.038	1.370
X90	T9	209	53.34	2802	2.381	2.371	4.384
X90	T10	210	5.334x10 ⁻³	2068	4.445	6.273	5.357
X90	T11	211	0.5334	2313	3.016	0.866	3.265
X90	T12	212	53.34	--	--	--	--
X90	L1	213	5.334x10 ⁻³	2580	2.883	1.057	3.850
X90	L2	214	0.5334	3025	3.810	1.051	2.146
X90	L3	215	53.34	4359	2.032	3.503	5.259
X90	L4	216	5.334x10 ⁻³	2936	2.667	1.696	4.678
X90	L5	217	0.5334	4003	3.810	2.335	10.434
X90	L6	218	53.34	5738	3.810	3.585	15.389
X90	L7	219	5.334x10 ⁻³	3203	4.763	1.584	10.739
X96	T8	220	5.334x10 ⁻³	2113	2.699	0.885	2.881
X96	T9	221	0.5334	2891	3.016	1.226	4.316
X96	T10	222	53.34	3692	2.477	1.121	3.839
X96	T11	223	5.334x10 ⁻³	2936	2.540	1.492	3.994
X96	T12	224	0.5334	4893	3.366	1.783	9.276
X96	L1	225	53.34	6032	3.175	2.001	7.355
X96	L2	226	5.334x10 ⁻³	4048	3.937	1.788	8.717

APPENDIX I (cont)
ENGINEERING DATA OBTAINED FROM RHESUS
MONKEY SINGLE VERTEBRAL BODIES

Specimen No.	VB No.	Displace. Rate (m/min)	Ult. Load (N)	Def. to Ult. Load (mx10 ⁻³)	Stiffness (N/mx10 ⁶)	Energy to Ult. Load (J)	
X96	L3	227	0.5334	4671	2.223	4.041	6.999
X96	L4	228	53.34	5516	2.527	5.004	3.921
X96	L5	229	5.334x10 ⁻³	4448	4.318	1.230	9.869
X96	L6	230	0.5334	5694	2.667	4.028	10.344
X96	L7	231	53.34	8452	5.398	3.713	30.834
34A	T8	232	5.334	1935	1.429	1.541	1.212
34A	T9	233	5.334x10 ⁻⁴	2157	5.080	0.711	6.799
34A	T10	234	5.334x10 ⁻²	2891	5.398	0.943	9.827
34A	T11	235	5.334	3648	4.604	1.611	11.462
34A	T12	236	5.334x10 ⁻⁴	2713	4.763	0.861	7.819
34A	L1	237	5.334x10 ⁻²	3737	4.763	1.907	12.835
34A	L2	238	5.334	5071	5.715	1.706	18.959
34A	L3	239	5.334x10 ⁻⁴	3781	6.350	1.868	17.451
34A	L4	240	5.334x10 ⁻²	4537	8.255	1.284	25.970
34A	L5	241	5.334	5204	4.572	1.500	12.530
34A	L6	242	5.334x10 ⁻⁴	3781	6.223	1.373	16.468
34A	L7	243	5.334x10 ⁻²	4671	6.668	1.541	21.173
584A	T8	244	5.334x10 ⁻²	2313	2.096	1.261	2.583
584A	T9	245	5.334	2580	1.588	1.821	1.840
584A	T10	246	5.334x10 ⁻⁴	2269	1.778	1.576	2.642
584A	T11	247	5.334x10 ⁻²	2713	2.858	1.051	3.632
584A	T12	248	5.334	3959	2.699	1.681	4.638
584A	L1	249	5.334x10 ⁻⁴	2758	2.159	1.560	2.949
584A	L2	250	5.334x10 ⁻²	3781	3.493	1.423	6.728
584A	L3	251	5.334	5115	3.493	1.842	9.756
584A	L4	252	5.334x10 ⁻⁴	3136	3.810	1.101	6.672
584A	L5	253	5.334x10 ⁻²	4181	4.445	1.479	11.988
584A	L6	254	5.334	5560	5.080	1.691	16.965
584A	L7	255	5.334x10 ⁻⁴	3247	8.128	0.881	10.214
882A	T8	256	5.334	--	--	--	--
882A	T9	257	5.334x10 ⁻²	--	--	--	--
882A	T10	258	5.334x10 ⁻⁴	2891	4.445	1.061	7.453
882A	T11	259	5.334x10 ⁻²	3914	3.175	1.910	7.604
882A	T12	260	5.334x10 ⁻⁴	3514	5.080	0.799	7.666
882A	L1	261	5.334	5783	5.080	1.416	17.982
882A	L2	262	5.334x10 ⁻⁴	3781	3.366	1.653	7.700
882A	L3	263	5.334	6850	3.937	3.121	16.383
882A	L4	264	5.334x10 ⁻²	5605	5.715	1.615	19.315
882A	L5	265	5.334x10 ⁻⁴	5471	6.985	1.217	22.563
882A	L6	266	5.334x10 ⁻²	6939	5.906	2.215	26.269
882A	L7	267	5.334	8007	5.080	2.802	25.681

APPENDIX I (Concluded)
ENGINEERING DATA OBTAINED FROM RHESUS
MONKEY SINGLE VERTEBRAL BODIES

Specimen No.	VB No.	Displace. Rate (m/min)	Ult. Load (N)	Def. to Ult. Load ($\text{mx}10^{-3}$)	Stiffness ($\text{N}/\text{mx}10^6$)	Energy to Ult. Load (J)
W92 T8	268	5.334×10^{-4}	867	2.159	0.458	0.859
W92 T9	269	5.334×10^{-2}	1223	2.191	0.631	1.637
W92 T10	270	5.334	1646	3.651	0.490	2.781
W92 T11	271	5.334×10^{-4}	1090	2.540	0.494	1.408
W92 T12	272	5.334×10^{-2}	1334	3.239	0.480	2.110
W92 L1	273	5.334	1913	2.858	1.090	3.197
W92 L2	274	5.334×10^{-4}	1601	4.572	0.457	4.000
W92 L3	275	5.334×10^{-2}	2535	4.445	0.978	7.355
W92 L4	276	5.334	2269	1.969	1.168	1.667
W92 L5	277	5.334×10^{-4}	1668	1.778	1.066	1.347
W92 L6	278	5.334×10^{-2}	1824	1.905	1.194	1.638
W92 L7	279	5.334	2402	1.588	1.5181.518	1.678

APPENDIX II

ENGINEERING DATA OBTAINED FROM RHESUS
MONKEY SINGLE VERTEBRAL BODIES

Specimen No.	VB No.	Displace. Rate (m/min)	Specimen Area (m ² x10 ⁻³)	Orig Length (mx10 ⁻²)	Ult. Eng. Stress (Pax10 ⁶)	Eng. Strain to Ult. Stress (m/m)	Elastic Modulus (Pax10 ⁶)
884A	T8	53.34	0.11	0.930	26.768	0.218	154.4
884A	T9	5.334x10 ⁻³	0.14	0.960	14.995	0.265	68.3
884A	T10	0.5334	0.14	1.069	---	---	---
884A	T11	53.34	0.15	1.217	26.294	0.159	370.4
884A	T12	5.334x10 ⁻³	0.18	1.293	18.621	0.182	132.0
884A	L1	0.5334	0.21	1.473	21.465	0.203	115.7
884A	L2	53.34	0.23	1.651	29.133	0.153	233.8
884A	L3	5.334x10 ⁻³	0.26	1.844	18.456	0.145	162.9
884A	L4	0.5334	0.25	1.996	22.517	0.111	279.9
884A	L5	53.34	0.27	2.146	29.850	0.112	429.3
884A	L6	5.334x10 ⁻³	0.29	2.210	17.966	0.144	156.9
884A	L7	0.5334	0.31	2.075	21.437	0.168	207.1
A104	T8	5.334x10 ⁻³	0.13	0.965	19.056	0.507	80.2
A104	T9	0.5334	0.16	1.016	21.457	0.469	82.8
A104	T10	53.34	0.16	1.102	21.669	0.161	188.9
A104	T11	0.5334	0.18	1.224	21.577	0.376	99.9
A104	T12	53.34	0.20	1.341	29.707	0.308	225.8
A104	L1	5.334x10 ⁻³	0.21	1.521	19.049	0.306	133.1
A104	L2	0.5334	0.23	1.674	25.177	0.266	247.5
A104	L3	5.334x10 ⁻³	0.24	1.730	19.987	0.294	123.2
A104	L4	53.34	0.25	1.918	29.163	0.232	305.7
A104	L5	5.334x10 ⁻³	0.25	2.019	21.644	0.302	172.7
A104	L6	53.34	0.26	1.948	30.756	0.293	172.8
A104	L7	0.5334	0.28	1.694	23.410	0.300	192.4

APPENDIX II (cont)

ENGINEERING DATA OBTAINED FROM RHESES
MONKEY SINGLE VERTEBRAL BODIES

Specimen No.	Specimen	VB No.	Displace. Rate (m/min)	Specimen Area (m ² x10 ⁻³)	Orig. Length (mx10 ⁻²)	Ult. Eng. Stress (Pax10 ⁶)	Eng. Strain to Ult. Stress (m/m)	Elastic Modulus (Pax10 ⁶)
X90	T8	208	0.5334	0.13	0.975	15.579	0.130	148.1
X90	T9	209	53.34	0.15	1.024	18.405	0.233	138.1
X90	T10	210	5.334x10 ⁻³	0.17	1.176	11.963	0.378	42.7
X90	T11	211	0.5334	0.22	1.265	10.545	0.238	50.0
X90	T11	212	53.34	0.23	1.488	---	---	---
X90	L1	213	5.334x10 ⁻³	0.26	1.562	9.874	0.185	63.2
X90	L2	214	0.5334	0.26	1.849	11.750	0.206	75.5
X90	L3	215	53.34	0.30	1.956	14.531	0.104	228.3
X90	L4	216	5.334x10 ⁻³	0.32	2.019	9.230	0.132	107.8
X90	L5	217	0.5334	0.33	2.131	12.215	0.179	151.9
X90	L6	218	53.34	0.34	2.164	16.941	0.176	229.0
X90	L7	219	5.334x10 ⁻³	0.31	1.958	10.257	0.243	99.3
X96	T8	220	5.334x10 ⁻³	0.14	0.963	14.621	0.280	58.9
X96	T9	221	0.5334	0.16	1.069	17.998	0.282	81.6
X96	T10	222	53.34	0.18	1.298	20.810	0.191	82.0
X96	T11	223	5.334x10 ⁻³	0.21	1.392	14.220	0.182	100.6
X96	T12	224	0.5334	0.25	1.476	19.497	0.228	104.8
X96	L1	225	53.34	0.27	1.664	22.638	0.191	125.0
X96	L2	226	5.334x10 ⁻³	0.26	1.862	15.454	0.211	127.1
X96	L3	227	0.5334	0.27	2.012	17.237	0.110	300.3
X96	L4	228	53.34	0.27	2.068	23.686	0.122	377.3
X96	L5	229	5.334x10 ⁻³	0.29	2.172	15.494	0.199	93.1
X96	L6	230	0.5334	0.32	2.154	18.048	0.124	274.8
X96	L7	231	53.34	0.33	2.007	25.486	0.269	224.6
34A	T8	232	5.334	0.12	1.024	15.703	0.140	128.0
34A	T9	233	5.334x10 ⁻⁴	0.14	1.095	15.699	0.464	56.7
34A	T10	234	5.334x10 ⁻²	0.17	1.275	16.912	0.423	70.3
34A	T11	235	5.334	0.18	1.438	20.559	0.320	130.6
34A	T12	236	5.334x10 ⁻⁴	0.20	1.641	13.835	0.290	72.0
34A	L1	237	5.334x10 ⁻²	0.22	1.816	17.288	0.262	160.3

APPENDIX II (cont)
ENGINEERING DATA OBTAINED FROM RHESES
MONKEY SINGLE VERTEBRAL BODIES

Specimen No.	VB No.	Displace. Rate (m/min)	Specimen Area (m ² x10 ⁻³)	Orig Length (mx10 ⁻²)	Ult. Eng. Stress (Pax10 ⁶)	Eng. Strain to Ult. Stress (m/m)	Elastic Modulus (Pax10 ⁶)
34A	L2	5.334	0.24	1.859	21.358	0.307	113.5
34A	L3	5.334x10 ⁻⁴	0.24	2.098	15.670	0.303	162.4
34A	L4	5.334x10 ⁻²	0.25	2.159	15.663	0.382	108.8
34A	L5	5.334	0.29	2.499	17.966	0.187	128.4
34A	L6	5.344x10 ⁻⁴	0.28	2.273	13.442	0.274	111.0
34A	L7	5.334x10 ⁻²	0.28	1.643	16.681	0.406	90.5
584A	T8	5.334x10 ⁻²	0.14	0.991	16.446	0.212	88.8
584A	T9	5.334	0.14	1.059	18.774	0.150	140.4
584A	T10	5.334x10 ⁻⁴	0.15	1.214	15.288	0.146	129.0
584A	T11	5.334x10 ⁻²	0.18	1.344	15.021	0.213	78.2
584A	T12	5.334	0.19	1.486	20.731	0.182	130.8
584A	L1	5.334x10 ⁻⁴	0.22	1.654	12.573	0.131	117.6
584A	L2	5.334x10 ⁻²	0.25	1.814	15.066	0.193	102.9
584A	L3	5.334 ⁻⁴	0.26	1.923	19.922	0.182	137.9
584A	L4	5.334x10 ⁻²	0.25	2.052	12.368	0.186	89.1
584A	L5	5.334x10 ⁻²	0.27	2.187	15.693	0.203	121.4
584A	L6	5.334	0.27	2.065	20.520	0.246	128.8
584A	L7	5.334x10 ⁻⁴	0.25	1.793	12.939	0.453	62.9
882A	T8	5.334	0.15	1.001	---	---	---
882A	T9	5.334x10 ⁻²	0.18	1.044	---	---	---
882A	T10	5.334x10 ⁻⁴	0.19	1.232	15.454	0.361	69.9
882A	T11	5.334x10 ⁻²	0.19	1.372	20.292	0.231	135.8
882A	T12	5.334x10 ⁻⁴	0.24	1.554	14.801	0.327	52.3
882A	L1	5.334	0.25	1.750	22.692	0.290	97.3
882A	L2	5.334x10 ⁻⁴	0.27	1.902	13.790	0.177	114.8
882A	L3	5.334	0.30	2.042	22.591	0.193	210.2
882A	L4	5.334x10 ⁻²	0.31	2.121	18.061	0.269	110.4
882A	L5	5.334x10 ⁻⁴	0.33	2.296	16.793	0.304	85.8
882A	L6	5.334x10 ⁻²	0.34	2.223	20.332	0.266	147.5
882A	L7	5.334	0.35	1.941	23.068	0.262	156.7

APPENDIX II (Concluded)

ENGINEERING DATA OBTAINED FROM RHESUS
MONKEY SINGLE VERTEBRAL BODIES

Specimen No.	VB No.	Displace. Rate (m/min)	Specimen Area ($m^2 \times 10^{-3}$)	Orig. Length ($m \times 10^{-2}$)	Ult. Eng. Stress ($Pax10^6$)	Eng. Strain to Ult. Stress (m/m)	Elastic Modulus ($Pax10^6$)
W92	T8	5.334×10^{-4}	0.12	0.945	7.307	0.228	36.4
W92	T9	5.334×10^{-2}	0.16	0.988	7.645	0.222	38.9
W92	T10	5.334	0.18	1.041	9.277	0.351	28.8
W92	T11	5.334×10^{-4}	0.21	1.212	5.312	0.210	29.2
W92	T12	5.334×10^{-2}	0.21	1.422	6.249	0.228	32.0
W92	L1	5.334	0.25	1.549	7.741	0.185	68.3
W92	L2	5.334×10^{-4}	0.26	1.765	6.159	0.259	31.1
W92	L3	5.334×10^{-2}	0.27	1.857	9.380	0.239	67.1
W92	L4	5.334	0.29	2.080	7.745	0.095	82.9
W92	L5	5.334×10^{-4}	0.31	2.037	5.409	0.087	70.4
W92	L6	5.334×10^{-2}	0.30	2.083	6.132	0.091	83.6
W92	L7	5.334	0.31	1.935	7.708	0.082	94.3

REFERENCES

1. Kazarian L., and Graves, G. "Compressive Strength Characteristics of the Human Vertebral Centrum"
SPINE, Vol. 2, Number 1, March 1977